Protein Structure and Folding:

Structure of the Hemoglobin-IsdH Complex Reveals the Molecular Basis of Iron Capture by *Staphylococcus aureus*

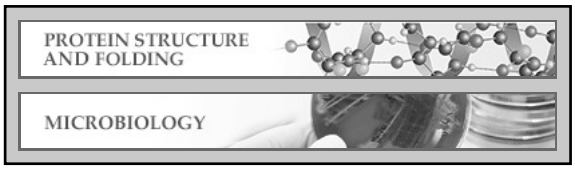

Claire F. Dickson, Kaavya Krishna Kumar, David A. Jacques, G. Reza Malmirchegini, Thomas Spirig, Joel P. Mackay, Robert T. Clubb, J. Mitchell Guss and David A. Gell

J. Biol. Chem. 2014, 289:6728-6738.
doi: 10.1074/jbc.M113.545566 originally published online January 14, 2014

THE JOURNAL OF BIOLOGICAL CHEMISTRY VOL. 289, NO. 10, pp. 6728–6738, March 7, 2014

Structure of the Hemoglobin-IsdH Complex Reveals the Molecular Basis of Iron Capture by *Staphylococcus aureus*[*] [◆]

Received for publication, December 23, 2013, and in revised form, January 12, 2014 Published, JBC Papers in Press, January 14, 2014, DOI 10.1074/jbc.M113.545566

Claire F. Dickson[‡], Kaavya Krishna Kumar[§1], David A. Jacques[§2], G. Reza Malmirchegini[¶3], Thomas Spirig[¶], Joel P. Mackay[§], Robert T. Clubb[¶], J. Mitchell Guss[§], and David A. Gell[‡4]

From the [‡]Menzies Research Institute Tasmania, University of Tasmania, Hobart, Tasmania 7000, Australia, the [§]School of Molecular Bioscience, University of Sydney, Sydney, New South Wales 2006, Australia, and the [¶]Department of Chemistry and Biochemistry, UCLA, Los Angeles, California 90095

Background: IsdB and IsdH proteins from *Staphylococcus aureus* strip heme iron from human hemoglobin.
Results: The IsdH·hemoglobin complex shows how globin-binding and heme-binding NEAT domains of IsdH cooperate to remove heme from both chains of hemoglobin.
Conclusion: The supradomain architecture of IsdH confers activity by precisely positioning the heme acceptor domain.
Significance: Multiple IsdH·hemoglobin interfaces may be targets for new antibiotics.

Staphylococcus aureus **causes life-threatening disease in humans. The *S. aureus* surface protein iron-regulated surface determinant H (IsdH) binds to mammalian hemoglobin (Hb) and extracts heme as a source of iron, which is an essential nutrient for the bacteria. However, the process of heme transfer from Hb is poorly understood. We have determined the structure of IsdH bound to human Hb by x-ray crystallography at 4.2 Å resolution, revealing the structural basis for heme transfer. One IsdH molecule is bound to each α and β Hb subunit, suggesting that the receptor acquires iron from both chains by a similar mechanism. Remarkably, two near iron transporter (NEAT) domains in IsdH perform very different functions. An N-terminal NEAT domain binds α/β globin through a site distant from the globin heme pocket and, via an intervening structural domain, positions the C-terminal heme-binding NEAT domain perfectly for heme transfer. These data, together with a 2.3 Å resolution crystal structure of the isolated N-terminal domain bound to Hb and small-angle x-ray scattering of free IsdH, reveal how multiple domains of IsdH cooperate to strip heme from Hb. Many bacterial pathogens obtain iron from human hemoglobin using proteins that contain multiple NEAT domains and other domains whose functions are poorly understood. Our results suggest that, rather than acting as isolated units, NEAT domains may be integrated into higher order architectures that employ multiple interaction interfaces to efficiently extract heme from host proteins.**

Staphylococcus aureus is a Gram-positive bacterial pathogen that causes infections of the skin and invasive disease in many tissues and organs. *S. aureus* is the leading cause of surgical site infections, skin and soft tissue infections, and infective endocarditis (1). Methicillin-resistant *S. aureus* strains that are resistant to all β-lactam antibiotics cause hospital- and community-acquired infections with high mortality rates (2, 3). New antibacterial treatments are urgently needed, but their development requires a better understanding of the mechanisms that underlie *S. aureus* pathogenesis.

Proteins displayed on the surface of pathogenic bacteria are at the frontline of the host-pathogen interface and interact with tissues of the host to carry out functions in adhesion, cell invasion, and acquisition of nutrients. Prominent among these functions is the capture of iron from the host (4). As well as being required at the active sites of many essential proteins, iron performs an important signaling role in pathogenesis and regulates the activation of nearly 400 *S. aureus* genes, including many required for colonization of the host (5). Under normal physiological conditions, all iron in the human body exists in complex with proteins. Successful pathogens have therefore evolved effective mechanisms to capture iron directly from these proteins. For example, Gram-negative pathogenic *Neisseria* species express the outer membrane transferrin-binding protein A (TbpA) and TbpB, which extract iron from serum transferrin (6). Hb is the most abundant iron source in humans, and many bacteria express proteins to capture this iron, such as iron-regulated surface determinant H (IsdH)[5] expressed on the surface of *S. aureus*.

In mammals, ~70% of the total body iron is iron protoporphyrin IX (heme) that is bound to Hb. *S. aureus* can obtain all of its iron requirements from Hb (7–9), which it gains access to by secreting hemolytic toxins that lyse erythrocytes. Hb is cap-

* This work was supported, in whole or in part, by National Institutes of Health Grant AI52217 (to R. T. C.). This work was also supported by the University of Tasmania (to D. A. G.).
◆ This article was selected as a Paper of the Week.
The atomic coordinates and structure factors (codes 4FC3 and 4IJ2) have been deposited in the Protein Data Bank (http://wwpdb.org/).
[1] Present address: Walter and Eliza Hall Institute of Medical Research, Parkville Victoria 3052, Australia.
[2] Present address: Medical Research Council (MRC) Laboratory of Molecular Biology, Francis Crick Avenue, Cambridge Biomedical Campus, Cambridge CB2 0QH, United Kingdom.
[3] Present address: Dept. of Pharmaceutical Chemistry, University of California, San Francisco, San Francisco, CA 94158.
[4] To whom correspondence should be addressed: Menzies Research Institute Tasmania, University of Tasmania, 17 Liverpool St., Hobart, TAS 7000, Australia. Tel.: 61-3-62264608; E-mail: david.gell@utas.edu.au.

[5] The abbreviations used are: IsdH, iron-regulated surface determinant H; NEAT, near iron transporter; SAXS, small angle x-ray scattering; r.m.s.d., root mean square deviation; Bis-Tris, 2-(bis(2-hydroxyethyl)amino)-2-(hydroxymethyl)propane-1,3-diol; Hal, heme-acquisition leucine-rich repeat protein; IlsA, iron-regulated leucine rich surface protein A; Shr, streptococcal hemoprotein receptor.

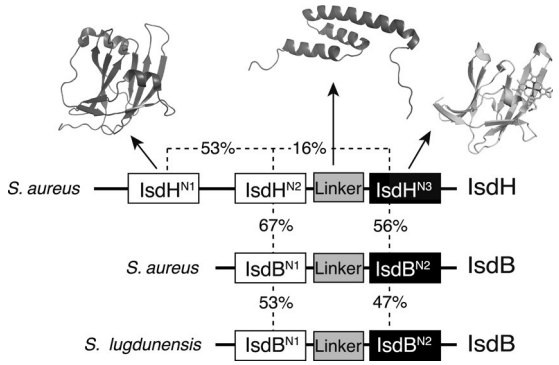

FIGURE 1. **Domain structure of IsdB and IsdH.** NEAT domains with Hb binding or heme binding activity are represented by *white* and *black boxes*, respectively, and sequence identity is indicated. Known structures of the isolated C-terminal NEAT domain (43), the helical linker (27), and the N-terminal NEAT domain (11) of IsdH are shown. IsdH shares a region of extended homology with IsdB, comprising $IsdH^{N2}$, the helical linker domain, and $IsdH^{N3}$ ($IsdH^{N2\text{-}N3}$).

tured onto the surface of *S. aureus* through the Hb receptors IsdB and IsdH (9–13), and heme is extracted via an unknown mechanism. The captured heme is then transferred to heme carrier proteins, IsdA and IsdC, which relay heme to the transmembrane heme permease complex, IsdE/F (14–18). IsdA, IsdB, IsdC, and IsdH are covalently attached to the bacterial peptidoglycan cell wall via a C-terminal amide linkage (19, 20). Members of the Isd pathway are the most highly up-regulated genes in *S. aureus* in response to iron starvation (5, 19–21), a condition that the bacteria experience during the early stages of an infection. Deletion of IsdH reduces *S. aureus* bacteremia in a mouse model (22), and deletion of IsdB protects against infections in heart (13, 23) and kidney (9, 24), indicating that Hb receptors have an important role in infection and that the Isd pathway might represent a therapeutic target for infections such as endocarditis, where *S. aureus* currently causes high mortality rates (25, 26).

The domain architectures of *S. aureus* IsdH and IsdB (Fig. 1) are similar, with an extended region of homology that includes all three recognized domains of IsdB, including two near iron transporter (NEAT) domains and a recently identified three-helix linker domain (27). A homologue of IsdB/H occurs in the related species *Staphylococcus lugdunensis* (28), which also causes infective endocarditis (29). Functionally related proteins that contain NEAT domains and capture heme from Hb are found in many Gram-positive bacteria including *Bacillus anthracis* (30–33), *Bacillus cereus* (34), and *Streptococcus pyogenes* (35). The C-terminal NEAT domain of IsdB/H (Fig. 1, *black boxes*) and NEAT domains in IsdA and IsdC (not shown) bind heme with nanomolar to subnanomolar affinity (12, 18, 27, 36–38). A transfer of heme between these domains occurs through formation of transient protein complexes (14, 16, 18, 36, 39–41). IsdB/H contain a second class of NEAT domains that bind to the Hb protein, but do not bind heme (Fig. 1, *white boxes*). The two N-terminal NEAT domains of IsdH ($IsdH^{N1}$ and $IsdH^{N2}$) bind to the α subunit of Hb with an affinity of 17–100 nM (10–12), and $IsdH^{N2}$ also binds β Hb, albeit with a lower affinity (11). Together, these binding activities allow IsdB and IsdH to capture heme from Hb at up to 500× the rate of simple heme dissociation from Hb chains (18, 27, 42). However, although the structures and ligand binding activities of the $IsdH^{N1}$, $IsdH^{N3}$, and $IsdB^{N2}$ NEAT domains are known (11, 12, 27, 39, 43), the isolated domains do not release or capture heme from Hb, and the heme capture process is still poorly understood.

Because individual domains do not recapitulate Hb-receptor function, we have analyzed a functional three-domain fragment of IsdH ($IsdH^{N2\text{-}N3}$; Fig. 1). Here we report the structures of $IsdH^{N2}$ and $IsdH^{N2\text{-}N3}$ in complex with Hb using x-ray crystallography, providing the first insights into how the domains of the Hb receptors of *S. aureus* cooperate to extract heme from Hb.

EXPERIMENTAL PROCEDURES

Protein Production—$IsdH^{N2}$ (residues 321–467), human Hb, and individual Hb chains were obtained as described previously (11). For x-ray crystallographic and SAXS studies, IsdH (residues 326–660) carrying a Tyr-642 to Ala mutation ($IsdH^{N2\text{-}N3(Y642A)}$) was expressed and purified as described previously (27). For heme transfer experiments, $IsdH^{N2\text{-}N3}$ (residues 321–655) and $IsdH^{N3}$ (residues 542–655) from *S. aureus* strain TCH1516 were cloned into pET15b (Novagen) for expression with an N-terminal hexahistidine tag. The proteins were expressed and purified to yield final products with the additional N-terminal sequence MGSSHHHHHHSSGLVPRGSHMLE. $IsdH^{N2\text{-}N3}$ was purified over immobilized metal affinity chromatography resin (HIS-Select Nickel Affinity Gel, Sigma). The load condition was 50 mM sodium phosphate, pH 7.4, 500 mM NaCl, 20 mM imidazole. The bound protein was washed in equilibration buffer containing 25 mM imidazole and eluted in 100 mM imidazole. Additional purification was performed by anion-exchange (Q-Sepharose, GE Healthcare); proteins were loaded in 10 mM sodium phosphate, pH 7.0, and eluted over a gradient of 100–250 mM NaCl. A final gel filtration step over a Superose 12 column (GE Healthcare Life Sciences) equilibrated in 150 mM sodium phosphate, pH 7.0, was performed.

X-ray Crystallography—Hb and $IsdH^{N2}$ were mixed together in 1:2 molar ratio (5 mg/ml Hb) and crystallized by hanging drop vapor diffusion. Crystallization conditions included 0.2 M sodium formate, 0.1 M Bis-Tris propane, pH 7.5, 20% (w/v) PEG3350, and produced crystals of 50–100 μm. The crystals were cryoprotected with 30% glycerol and flash-cooled in a cold nitrogen stream (100 K). Diffraction data to 2.3 Å resolution were collected at 100 K with an x-ray beam wavelength of 0.95370 Å at the Micro Crystallography MX2 beamline at the Australian Synchrotron (Clayton, Australia). Data were indexed and scaled using HKL2000 and SCALEPACK (44), respectively. The structure was solved by molecular replacement using PHASER (45), which gave a unique solution when using $\alpha{\cdot}\beta$ Hb dimer (Protein Data Bank (PDB) code 2DN1) and an alanine model of $IsdH^{N1}$ (PDB code 3SZK) generated by CHAINSAW (46) as independent search models. The structure was refined using REFMAC5 (47), with manual map inspection and model building being performed in COOT (48). The quality of the model was regularly checked for steric clashes, incorrect stereochemistry, and rotamer outliers using MolProbity (49). The final structure had 98.57% of residues in the Ramachandran preferred region, with no outliers according to MolProbity. Coordinates and structure factors can be found at

Research Collaboratory for Structural Bioinformatics (RCSB) PDB entry 4FC3.

The IsdH$^{N2\text{-}N3(Y642A)}$·Hb complex was buffer-exchanged into 20 mM HEPES, pH 7.5, and crystallized by hanging drop vapor diffusion. Crystals of 200–500 μm grew in 0.2 M diammonium citrate, 13% (w/v) PEG3350, 0.7% 1-butanol, pH 4.6, at 294 K. Crystals were cryoprotected in stabilizing solution containing 25% ethylene glycol before flash freezing in liquid nitrogen. Diffraction data to 4.2 Å resolution were collected at 100 K with an x-ray beam wavelength of 0.95369 Å on the Australian Synchrotron MX2 beamline. Integration and scaling were performed with HKL-2000 and SCALEPACK (44). Molecular replacement was performed with PHASER (45) using the crystal structures of Hb (PDB 3P5Q), IsdH^{N2} (PDB 4FC3), and IsdH^{N3} (PDB 2E7D and 2Z6F) as search models. Clear regions of helical density corresponding to the helical linker domain, which was left out of molecular replacement, provided confidence in the experimental model. The NMR structure of the linker (PDB 2LHR) (27) was placed manually into the model. Anomalous signal was observed at the predicted positions of the iron atoms in the heme groups coordinated by the four globin chains. Although the IsdH^{N2} and IsdH^{N3} domains are structurally similar, PHASER unambiguously placed them in unique locations within the complex. The solution was refined with Buster version 2.10.0 (50). Refinement was weighted heavily toward the geometry of the high-resolution structures used for molecular replacement, and included noncrystallographic symmetry restraints (51) and translation/liberation/screw refinement (groups were defined as single domains). Difference electron density joining the domains of IsdH indicated the positions of linking residues, but these could not be built with confidence and so were not included in the model. MolProbity (49) was used to verify the geometry, and the Ramachandran statistics are as follows; 96.2% of residues were found in favored regions; 99.9% were found in allowed regions; 0.06% were found in disallowed regions. Coordinates and structure factors can be found at RCSB PDB entry 4IJ2.

SAXS—Samples of IsdH$^{N2\text{-}N3(Y642A)}$ were buffer-exchanged by gel filtration to obtain matched buffer controls. SAXS data were collected on an Anton Paar SAXSess instrument with a sealed tube source. $I(0)$ values and $P(r)$ curves were calculated using GIFT (Anton Paar, Graz, Austria) and PRIMUS (72), and experimental molecular weights were calculated from the calibrated $I(0)$ values (52). No significant aggregation or interparticle interference was found by Guinier or $P(r)$ analysis. *Ab initio* shape reconstruction from the experimental scattering data was carried out using DAMMIF (53), and 10 independent models were averaged using DAMAVER (54). Although there was some variation between the models (normalized spatial discrepancy = 0.983), no outliers were identified, and filtering of the average envelope to retain the most highly occupied area gave a dumbbell-shaped envelope, which was superposed with the IsdH$^{N2\text{-}N3}$ crystal structure using SUPCOMB (55).

Heme Transfer—Heme transfer was monitored by UV-visible spectroscopy. Apo-IsdH$^{N2\text{-}N3}$ was produced using the acid acetone heme extraction method of Ascoli *et al.* (56). Apo-IsdH$^{N2N3(Y642A)}$ was obtained heme-free upon purification from *Escherichia coli*. Hb samples were converted to ferric Hb (Hb containing ferric heme), a form of Hb that is produced following lysis of red blood cells, by the addition of a 5-fold molar excess of potassium ferricyanide and monitored using UV-visible spectrophotometry. Excess oxidant was removed by buffer-exchange over G-25 Sepharose (GE Healthcare). Hb was mixed with apo-IsdH$^{N2\text{-}N3}$ at the ratios indicated under "Results." Reactions were performed in 150 mM sodium phosphate, pH 7.0, at 4 °C. Absorbance spectra (350–700 nm) were recorded at 40-s intervals on a JASCO UV-630 spectrophotometer equipped with a temperature-controlled sample chamber. To determine the percentage of heme transferred from Hb to the Isd protein at each time point, the acquired UV-visible spectrum was fit to a linear combination of ferric Hb and fully heme-loaded holo-IsdH$^{N2\text{-}N3}$ spectra.

TABLE 1
Data collection and refinement statistics (molecular replacement)
Diffraction data were collected from a single crystal in each case. Values in parentheses are for highest-resolution shell.

	IsdH^{N2}·Hb	IsdH$^{N2\text{-}N3(Y642A)}$·Hb
Data collection		
Space group	$C222_1$	$P2_12_12$
Cell dimensions		
a, *b*, *c* (Å)	67.04, 149.85, 86.26	132.90, 185.30, 103.21
α, β, γ (°)	90, 90, 90	90, 90, 90
Resolution (Å)	50.0-2.26 (2.26-2.32)	49.7-4.23 (4.24-4.32)
R_{merge} (%)	12.2 (57.3)	9.2 (72.7)
$I/\sigma I$	12.5 (2.3)	10.17 (1.83)
Completeness (%)	93.2 (93.2)	99.9 (100)
Redundancy	3.8 (3.5)	3.8 (3.8)
Refinement		
Resolution (Å)	49.9-2.26	29.15-4.24
No. of reflections	19,451	18,511
R_{work}/R_{free}	0.219/0.256	0.299/0.310
No. of atoms		
Protein	3282	13,375
Ligand/ion	96	172
Water	30	
B-factors		
Protein	24.63	86.14
Ligand/ion	17.94	65.65
Water	21.56	
r.m.s.d. values		
Bond lengths (Å)	0.005	0.008
Bond angles (°)	0.760	0.84

RESULTS

IsdH^{N2} Binds to a Site Comprising Portions of the A and E Helices of α Hb—To begin to understand the function of IsdH$^{N2\text{-}N3}$, we crystallized an IsdH^{N2}·Hb complex from a mixture containing a 2:1 molar ratio of IsdH^{N2} to Hb tetramer and determined the x-ray crystal structure to 2.3 Å resolution (Table 1 and Fig. 2). Phases were obtained by molecular replacement using the structures of Hb (PDB 2DN1) (57) and IsdH^{N1} (PDB 3SZK) (11). The asymmetric unit of the IsdH^{N2}·Hb crystals comprises one Hb dimer with one IsdH^{N2} molecule bound to the α Hb subunit (Fig. 2*A*). IsdH^{N2} (Fig. 2*B*) binds in the same position on α Hb as IsdH^{N1} (Fig. 2*C*), and a comparable number of residues at both interfaces participate in hydrogen bonds and salt bridges, including interactions with Asp-74, Lys-11, and Thr-8 of α Hb (Fig. 2, *B* and *C*). A short α helix in IsdH^{N2} (primary sequence FYHYAS), containing a series of aromatic side chains, forms part of the IsdH^{N2}·α Hb-binding interface (Fig. 2*D*). A helix with similar hydrophobic character, but different primary sequence (YYHFFS), occurs in IsdH^{N1} (11, 12). A Phe side chain from a different position in the IsdH^{N2} or

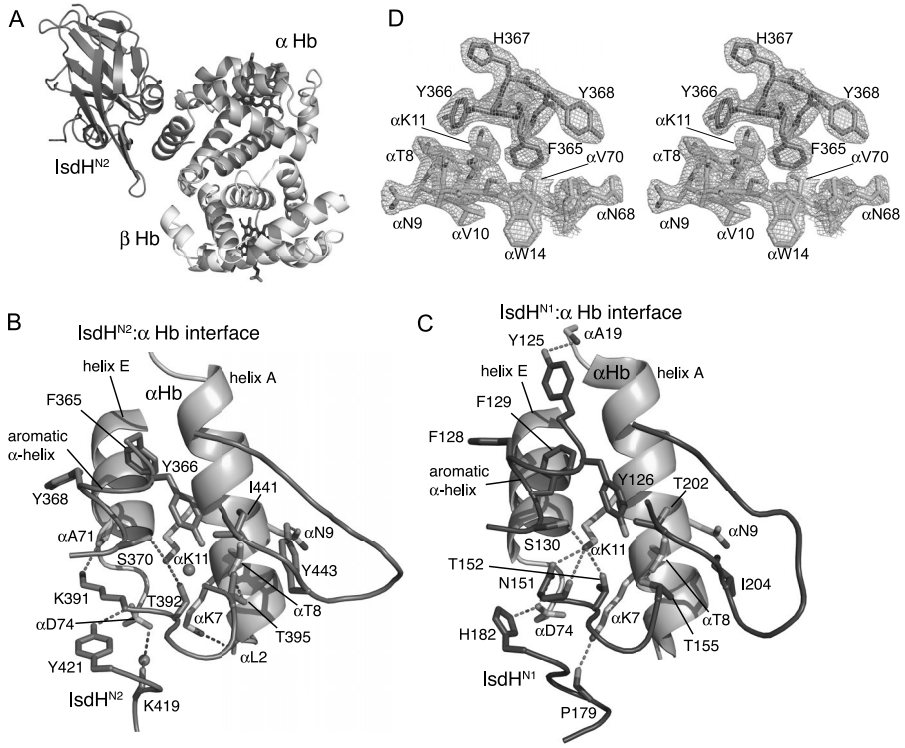

FIGURE 2. **Structure of the IsdH^{N2}·Hb complex.** *A*, the crystal structure of IsdH^{N2} bound to Hb (PDB 4FC3) contains one molecule of IsdH^{N2} and one α·β heterodimer in the asymmetric unit. In the crystal, two α·β dimers generate an Hb tetramer with an R2 quaternary structure (71). *B*, interaction interface of IsdH^{N2} (*blue*) with α Hb (*orange*). Side chains that contribute to the molecular interface are shown in stick representation. *C*, interaction interface of IsdH^{N1}·α Hb (PDB 3SZK) (11), showing a number of conserved interactions with the IsdH^{N2}·α Hb interface. *D*, stereo diagram of part of the IsdH^{N2}·Hb interface including the aromatic IsdH^{N2} helix (*blue*), showing the $2F_o - F_c$ electron density map contoured at 1 σ.

IsdH^{N1} aromatic α helix is buried in the groove between helices A and E of α Hb (Fig. 2, *B* and *C*), suggesting that the aromatic motif is functionally conserved. The α Hb subunit retains its native structure in complex with either IsdH^{N2} (r.m.s.d. of 0.8 Å over 136 Cα atoms as compared with PDB 2DN1) or IsdH^{N1} (r.m.s.d. of 0.8 Å over 136 Cα atoms as compared with PDB 2DN1), which suggests that the IsdH^{N1} and IsdH^{N2} domains alone do not destabilize the α globin fold or promote heme release, in agreement with previous functional studies (11, 27). In addition, the IsdH^{N2}-binding site is distant from the entrance to the globin heme pocket, making it unlikely to be directly involved in heme extraction. We conclude that IsdH^{N2} performs an Hb recognition/targeting role within the native IsdH receptor.

The Three Domains of IsdH$^{N2\text{-}N3}$ Are Assembled into a Higher Order Structure That Binds to α and β Hb Chains and Positions the Globin Heme Pocket to Achieve Heme Transfer—To trap a stable IsdH$^{N2\text{-}N3}$·Hb complex for x-ray crystallographic studies, we expressed IsdH$^{N2\text{-}N3}$ with a Tyr-642 to Ala mutation in the heme pocket of the IsdH^{N3} domain (IsdH$^{N2\text{-}N3(Y642A)}$); this inhibits heme binding (27). IsdH$^{N2\text{-}N3(Y642A)}$ was mixed with ferric human Hb at a 2:1 molar ratio and subject to extensive crystallization trials. X-ray diffraction data were collected to 4.2 Å resolution using synchrotron radiation (Table 1), and the structure (Fig. 3*A*) was solved using molecular replacement by searching in a stepwise fashion for domains using the crystal structures of Hb (PDB 3P5Q) (58), IsdH^{N2} (PDB 4FC3), and IsdH^{N3} (PDB 2E7D and 2Z6F) (43) as search models.

In the IsdH$^{N2\text{-}N3(Y642A)}$·Hb complex, each α or β Hb globin chain is bound independently by one IsdH$^{N2\text{-}N3(Y642A)}$ receptor molecule (Fig. 3*A*). The three domains of the receptor are arranged in a dumbbell structure with the globular IsdH^{N2} and IsdH^{N3} domains separated in space by the intervening helical linker domain (Fig. 3*B*). This arrangement is consistent with interdomain interactions detected in an NMR spectroscopic analysis of the free receptor (27). Despite differences in the α and β Hb chain sequences, IsdH is clearly bound to equivalent sites on both globin subunits (Fig. 3*C*). On the α subunit, the IsdH^{N2} domain docks in the same position in the IsdH$^{N2\text{-}N3(Y642A)}$·Hb and IsdH^{N2}·Hb structures, suggesting that the Hb-targeting function of IsdH^{N2} is preserved in the context of the full IsdH receptor and providing independent validation of both structures. At the IsdH$^{N2\text{-}N3(Y642A)}$·β interface, the IsdH^{N2} domain binds at a site on the A and E helices of β Hb, analogous to the binding site on α Hb. Of the 15 residues that comprise the IsdH^{N2}-interacting face of α Hb, there are three nonconservative substitutions in β Hb: αAla-5 is substituted by βGlu-6; αAsn-9 is substituted by βAla-10; and αLys-11 is substituted by βThr-12. The latter two changes are expected to disrupt hydrogen-bonding interactions with IsdH^{N2} (Fig. 2*B*). Nevertheless, interactions between isolated IsdH^{N2} and β Hb can be detected in gel filtration (11), suggesting that the IsdH$^{N2\text{-}N3(Y642A)}$·Hb crystal captures a weak mode of interaction that is mechanistically important (as described below).

In three of the IsdH receptor molecules, the helical linker domain positions the IsdH^{N3} domain directly over the heme

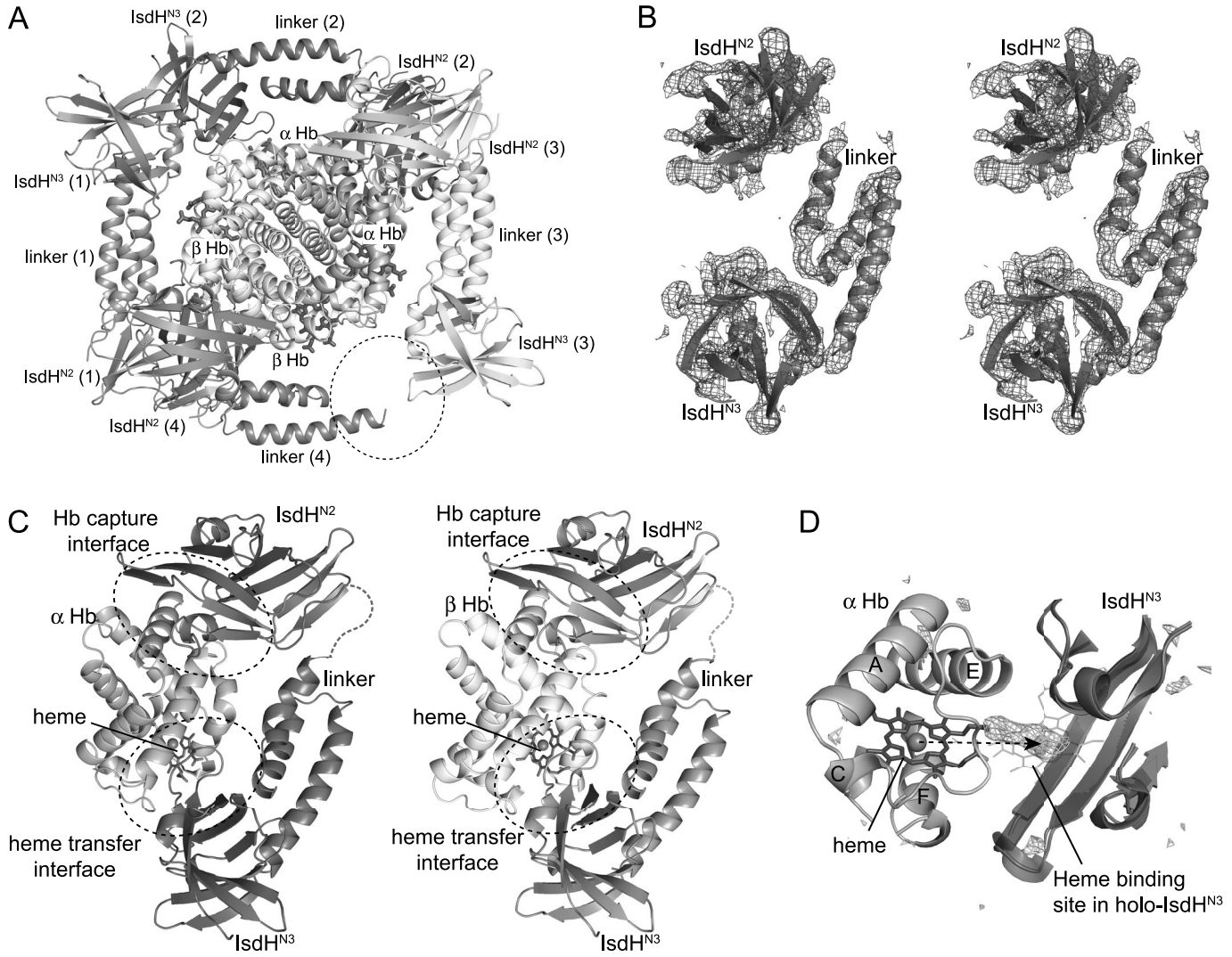

FIGURE 3. **Crystal structure of IsdH$^{N2\text{-}N3}$ bound to Hb.** *A*, four IsdH$^{N2\text{-}N3}$ receptors bind to one Hb tetramer in the asymmetric unit of the crystal (PDB 4IJ2). Three of the IsdH$^{N2\text{-}N3}$ receptors are complete, comprising IsdH^{N2}, linker, and IsdH^{N3} domains. The position of the IsdH^{N3} domain in the fourth receptor molecule is not well defined (the expected location is marked by a *dashed ellipse*). *B*, stereo diagram showing the $2F_o - F_c$ electron density map for one full IsdH$^{N2\text{-}N3}$ receptor contoured at 1 σ. *C*, detail of the IsdH$^{N2\text{-}N3}$·α (*blue/orange*) and IsdH$^{N2\text{-}N3}$·β (*teal/yellow*) interaction complexes. Residues from the loop regions, which are not modeled in the structure, are shown with *dashed lines*. *D*, the IsdH^{N3}·α interface with $F_o - F_c$ difference map shown at 3 σ (*green*), indicating electron density that is not accounted for by atoms of the IsdH$^{N2\text{-}N3}$·Hb model. The structure of heme-bound IsdH^{N3} (PDB 2Z6F, *red*) is superimposed to indicate the expected binding position of the heme group (*lines*), which coincides with a peak of $F_o - F_c$ difference electron density in the IsdH$^{N2\text{-}N3}$·Hb complex (*green*). Heme transfer from globin to the IsdH receptor requires a relatively small translation of only 12 Å between the E and F helices of the globin (*dashed arrow*).

pocket of the bound globin subunit. The electron density observed for the fourth IsdH^{N3} domain, which was expected to lie over the heme pocket of the other β Hb subunit, was not sufficiently strong to place this IsdH^{N3} domain with confidence (Fig. 3*A*, *dashed circle*), and it was therefore not included in the model. The three complete IsdH$^{N2\text{-}N3(Y642A)}$ molecules in the complex have essentially identical structures (backbone r.m.s.d. <1.2 Å in pairwise comparisons), indicating that, in addition to binding the same site on α and β Hb, IsdH$^{N2\text{-}N3}$ binds both globin chains in the same conformation (Fig. 3*C*). In this conformation, the IsdH^{N3} domain is positioned directly over the heme pocket on the globin, such that the heme would need to move only ~12 Å, through the entrance to the globin heme pocket, to effect transfer to IsdH (Fig. 3*D*, *dashed arrow*). Interestingly, electron density at the heme-binding site of the IsdH^{N3} domains (Fig. 3*D*, *green*), together with weak anomalous signal, suggests that the receptors have partial heme occupancy despite the inactivating Tyr-642 to Ala mutation. At the resolution of our x-ray data, however, it is not possible to say whether the globin heme pocket structure is altered by interaction with IsdH^{N3}. In addition, the heme-binding β strands (residues Val-637-Gln-645) of IsdH^{N3} are not well defined in the electron density. As a result, we are not able to discern whether localized structural changes occur in Hb to promote heme transfer. Nevertheless, the close proximity of IsdH and Hb heme-binding sites in the IsdH$^{N2\text{-}N3}$·Hb complex is consistent with a direct protein-to-protein heme relay.

The Three Domains of IsdH$^{N2\text{-}N3}$ Are Pre-organized to Position the Heme Acceptor Site over the α/β Hb Heme Pocket—To investigate whether changes in IsdH$^{N2\text{-}N3}$ conformation occur upon binding to Hb, we performed SAXS on the free IsdH$^{N2\text{-}N3(Y642A)}$ receptor. Model-free analysis of the SAXS

TABLE 2
Molecular parameters from SAXS

	$IsdH^{N2\text{-}N3(Y642A)}$	$IsdH^{N2\text{-}N3(Y642A)}$	$IsdH^{N2\text{-}N3(Y642A)}$
Structural parameters			
Sample concentration (mg/ml)	7	4.5	3
$I(0)$ (cm^{-1}) ($P(r)$ analysis)[a]	0.1770	0.1186	0.0807
$I(0)$ (cm^{-1}) ($P(r)$ analysis)[b]	0.183 ± 0.001	0.122 ± 0.001	0.0821 ± 0.0006
R_g (Å) ($P(r)$ analysis)[a]	27.75	28.96	28.99
R_g (Å) ($P(r)$ analysis)[b]	28.1 ± 0.2	30.4 ± 0.2	30.2 ± 0.02
$I(0)$ (cm^{-1}) (Guinier analysis)[b]	0.183 ± 0.001	0.121 ± 0.001	0.082 ± 0.001
R_g (Å) (Guinier analysis)[b]	27.7 ± 0.4	29.5 ± 0.5	29.6 ± 0.8
D_{max} (Å)[a]	85	90	85
Molecular mass determination			
Partial specific volume ($cm^3\ g^{-1}$)	0.732	0.732	0.732
Contrast ($\Delta\rho \times 10^{10}\ cm^{-2}$)	2.808	2.808	2.808
Molecular mass M_r (from $I(0)$)[a]	36,405	36,830	38,470
Molecular mass M_r (from $I(0)$)[b]	37,639	37,575	39,090
M_r calculated from primary sequence (monomer)	38,788	38,788	38,788

[a] Values generated with GIFT.
[b] Values generated with PRIMUS.

data yielded the expected molecular weights for all samples, which were within 10% of the theoretical molecular weights calculated from the sequences (Table 2). We generated theoretical scattering curves for the three full receptors present in the complex with Hb using the program CRYSOL (59). These theoretical curves fit extremely well to the solution scattering of $IsdH^{N2\text{-}N3(Y642A)}$, with χ values of 0.924, 0.904, and 0.866 (Fig. 4*A*), indicating that no major structural change occurs upon receptor binding and providing independent validation of the 4.2 Å resolution crystal structure. *Ab initio* shape reconstruction of the free IsdH receptor reveals close agreement with the crystal structure of the Hb-bound receptor (Fig. 4*B*). These results argue strongly that the receptor does not undergo a major conformational change upon binding to Hb. Instead, the domains of the receptor are pre-organized to position the heme acceptor site over the globin heme pocket.

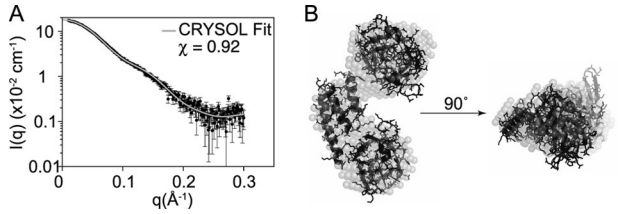

FIGURE 4. **The domain organization of $IsdH^{N2\text{-}N3}$ in solution is the same as that shown in the crystal structure.** *A*, fit of the experimental solution scattering of free $IsdH^{N2\text{-}N3}$ to the theoretical scattering curve generated for a single $IsdH^{N2\text{-}N3}$ molecule from the crystal structure of the complex with Hb (chain F of PDB 4IJ2). *B*, *ab initio* shape reconstruction of the $IsdH^{N2\text{-}N3}$ receptor (*spheres*), overlaid with the crystal structure of $IsdH^{N2\text{-}N3}$ (*ribbon* and *sticks*).

$IsdH^{N2\text{-}N3}$ Acquires Heme from α and β Hb—The structure of the $IsdH^{N2\text{-}N3}$·Hb complex shows how IsdH could access heme in both the α and the β subunits of Hb. Physical interaction between $IsdH^{N2}$ and isolated α and β Hb subunits has been demonstrated in solution, with the binding to β Hb being considerably weaker (11). To investigate whether $IsdH^{N2\text{-}N3}$ can remove heme from α and β chains of Hb, and hence probe the functional significance of β chain interactions, we studied the transfer of the heme from ferric Hb to apo-$IsdH^{N2\text{-}N3}$ using UV-visible spectroscopy. In the absence of heme, apo-$IsdH^{N2\text{-}N3}$ shows negligible absorption from 350–750 nm (Fig. 5*A*, *dashed line*). Holo-$IsdH^{N2\text{-}N3}$, when bound to ferric heme (Fig. 5*A*, *dotted* and *dashed line*), has a characteristic spectrum that distinguishes it from ferric Hb (Fig. 5*A*, *solid line*). After mixing ferric Hb with apo-$IsdH^{N2\text{-}N3}$, UV-visible spectra were acquired as a function of time, and the fraction of ferric Hb and holo-$IsdH^{N2\text{-}N3}$ at each time point was determined by least squares fitting to a linear combination of the spectra shown in Fig. 5*A*. At a mixing ratio of 5 apo-$IsdH^{N2\text{-}N3}$ to 1 Hb tetramer, there was rapid and quantitative transfer of heme from Hb to $IsdH^{N2\text{-}N3}$, with only ~5% ferric Hb remaining after 10 min at 4 °C (Fig. 5*B*, *bottom*, *dotted* and *dashed curve*). As an alternative approach to assess the number of Hb heme groups accessed by $IsdH^{N2\text{-}N3}$, we measured the final UV-visible spectrum after a 10-min incubation of ferric Hb with different amounts of apo-$IsdH^{N2\text{-}N3}$. We observed a linear relationship between apo-$IsdH^{N2\text{-}N3}$:Hb molar mixing ratio and the total spectral change at 406 nm, up to a molar ratio of ~3.5:1 (Fig. 5*C*), which was consistent with a 4:1 $IsdH^{N2\text{-}N3}$:Hb interaction model. Together, these experiments show that heme is effectively removed from both α and β chains under these conditions.

Although IsdH can quantitatively deplete heme from Hb, it is possible that heme is released into solution from destabilized Hb and scavenged by $IsdH^{N2\text{-}N3}$ receptors that are not physically bound to Hb chains. To investigate whether a physical interaction between the IsdH receptor and Hb is required to extract heme from all sites (α and β chains), we utilized the isolated $IsdH^{N3}$ heme-binding domain. The isolated $IsdH^{N3}$ domain is fully functional to bind heme from solution but is unable to capture heme from ferric Hb over the course of 10 min (Fig. 5*B*, *gray circles*), as shown previously by Spirig *et al.* (27). When $IsdH^{N2\text{-}N3}$ was mixed with Hb in a 2:1 ratio, in the presence or absence of additional $IsdH^{N3}$, the heme transfer curves were identical, with ~50% of heme groups removed from Hb in each case (Fig. 5*B*, compare *dashed* and *solid curves*), indicating that $IsdH^{N3}$ only captures heme from Hb in the context of the intact receptor. The absence of any detectible competition for heme binding between $IsdH^{N3}$ and $IsdH^{N2\text{-}N3}$ confirms that interaction between free $IsdH^{N3}$ and the globin heme pocket is extremely weak in the absence of the $IsdH^{N2}$ domain. Together, the above data indicate that heme extraction from Hb (i) takes place directly within an IsdH·Hb complex, (ii) requires contacts mediated through the $IsdH^{N2}$ domain, and

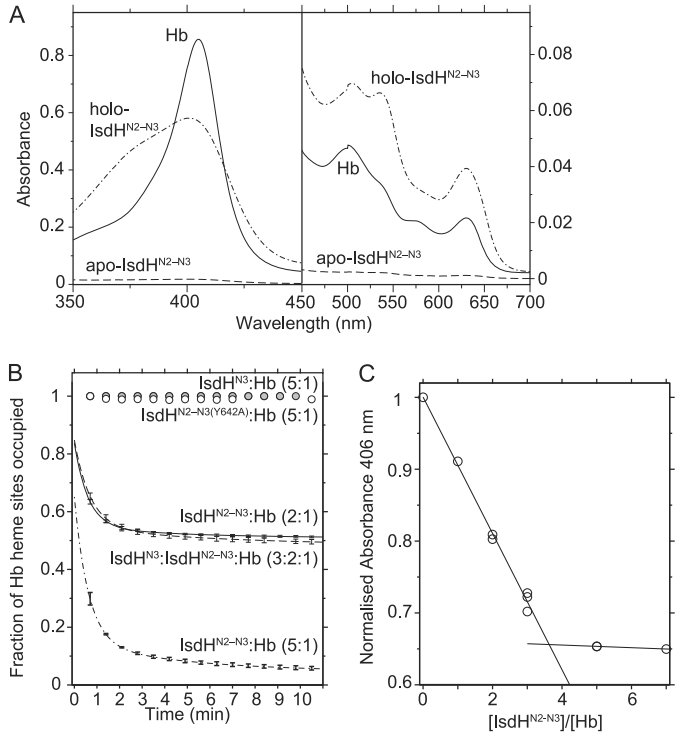

FIGURE 5. **Heme transfer from Hb to IsdH^{N2-N3}.** *A*, UV-visible absorption spectra of ferric Hb (6 μM heme, corresponding to 1.5 μM Hb tetramer), holo-IsdH^{N2-N3} (7.5 μM), and apo-IsdH^{N2-N3} (7.5 μM), showing that they are distinct. *B*, a time course showing the percentage of heme remaining bound to ferric Hb (1.5 μM) after mixing with apo-IsdH, as calculated by fitting a spectrum acquired at each time point to a combination of the spectra shown in *A*. Neither isolated IsdH^{N3} (*gray circles*) nor IsdH$^{N2-N3(Y642A)}$ (*white circles*) can acquire heme from Hb during the time course. A 2:1 molar mixture of IsdH^{N2-N3}:Hb resulted in depletion of ~50% of heme sites in Hb, corresponding to the transfer of 2 hemes per Hb tetramer (*solid curve*). At 5:1 IsdH^{N2-N3}:Hb, ~95% of heme is transferred (*dot-dashed curve*). The transfer is rapid, being essentially complete after 10 min at 4 °C. Heme transfer in a 3:2:1 molar mixture of IsdH^{N3}:IsdH^{N2-N3}:Hb (*dashed curve*) was very similar to that of 2:1 IsdH^{N2-N3}:Hb. *Error bars* are ± S.E. from two experiments. *C*, the plot shows absorbance at 406 nm, recorded after a 10-min incubation of apo-IsdH^{N2-N3}·Hb, prepared at different molar mixing ratios. The linear relationship between spectral change and IsdH^{N2-N3}:Hb ratio is consistent with a model in which 3–4 IsdH^{N2-N3} molecules interact with four heme sites per Hb tetramer.

(iii) occurs at both α and β Hb subunits, as predicted by the IsdH^{N2-N3}·Hb crystal structure.

DISCUSSION

We demonstrate here how multiple domains in IsdH cooperate to effect heme extraction from Hb. Excellent agreement between the IsdH^{N2-N3}·Hb crystal structure and the solution x-ray scattering of the free receptor indicates that the three domains of IsdH^{N2-N3} are pre-organized to position IsdH^{N3} at the entrance to the globin heme pocket when the IsdH^{N2} domain docks with its cognate site between the A and E helices of α or β Hb. The isolated heme-binding IsdH^{N3} domain interacts with Hb too weakly to function in heme uptake, indicating that physical positioning of this domain in the context of the intact receptor is an essential feature of the heme transfer mechanism. A high level of sequence homology between IsdH^{N2-N3}, IsdB, and an IsdB homologue from the related pathogen *S. lugdunensis* (28) indicates that our results are relevant to all three proteins.

Heme is extracted from Hb and moved across the bacterial cell wall to the bacterial membrane in a series of direct protein-to-protein transfer steps (Fig. 6). Transport by protein-to-protein relay is frequently employed in nature to transfer reactive species or signaling molecules in both prokaryote and eukaryote cells. Examples include copper transport (60), electron transport (61), and relay of phosphoryl groups in signal transduction in plants (62), animals (63), and bacteria (64). In these examples, precise positioning of the donor and acceptor proteins is critical to cargo transfer, and both donor and acceptor proteins have co-evolved to perform efficient ligand transfer. In contrast, Hb has evolved to minimize heme dissociation, and partial unfolding of the globin is required in order for heme to enter/exit the globin heme pocket (65). We speculate that the challenge of extracting heme from the deep binding cleft in Hb cannot be met by interaction through a single interface. Hence, the IsdB/H receptors are anchored through a site distant from the heme pocket (Fig. 6, *step 1*), which holds the IsdH^{N3} domain in contact with Hb while at the same time allowing conformational changes in the heme pocket to take place (Fig. 6, *step 2*). Consistent with this idea, mutagenesis studies of the Hb receptor A (HgbA) from Gram-negative *Haemophilus ducreyi* indicate that there is likewise a physical separation of the Hb-binding and heme uptake interfaces (66, 67). This similarity suggests that an architecture involving multiple interaction interfaces might have a functional advantage for heme extraction from Hb in a range of systems.

Protein-protein interactions that mediate transport or signaling are typically extremely transient in nature (60, 61, 64). In the Isd pathway, weak interactions ($K_d > 5$ mM) are responsible for rapid heme transfer between *S. aureus* IsdA and IsdC (41). The structure of IsdH^{N2-N3} predicts that the IsdB/H receptors would need to dissociate from Hb to relay heme to IsdA/C (Fig. 6, *step 3*), and hence there is necessarily a balance between the IsdB/H·Hb complex persisting long enough for heme extraction, but not so long that transfer to IsdA/C becomes impractically slow. In this light, it is possible that weaker binding of IsdH to β Hb, as compared with α Hb, is an adaptation to the intrinsically more rapid heme dissociation from the β subunits of Hb dimers/tetramers (42). Notably, IsdH contains an additional N-terminal Hb-binding domain, IsdH^{N1}, which is not present in IsdB. IsdH^{N1} and IsdH^{N2} bind to the same site on α Hb and so may compete for binding under some circumstances. IsdH^{N1} displays no detectible interaction with β Hb (11) and so is not expected to interfere with IsdH^{N2-N3} binding to β Hb. The precise role that IsdH^{N1} plays, in the context of full-length IsdH, will now need to be established. Notwithstanding these factors, our data indicate that heme capture by IsdH and IsdB occurs by a similar mechanism for α and β chains. Kinetic data also support a single mechanism of heme uptake from α and β chains; Zhu *et al.* (18) showed that heme is almost completely transferred from Hb to IsdB in under 2 min at 22 °C with a single rate constant.

In IsdH and IsdB, the same NEAT domain fold has evolved to specifically and exclusively bind either the surface of Hb or a heme molecule. The Pfam protein fold database identifies over 2000 NEAT domain sequences in Gram-positive species across the phylum *Firmicutes*, including many pathogens that cause severe human disease such as *S. pyogenes*, *B. anthracis*, *C. perfringens*, and *L. monocytogenes*, as well as *S. aureus*. Most NEAT

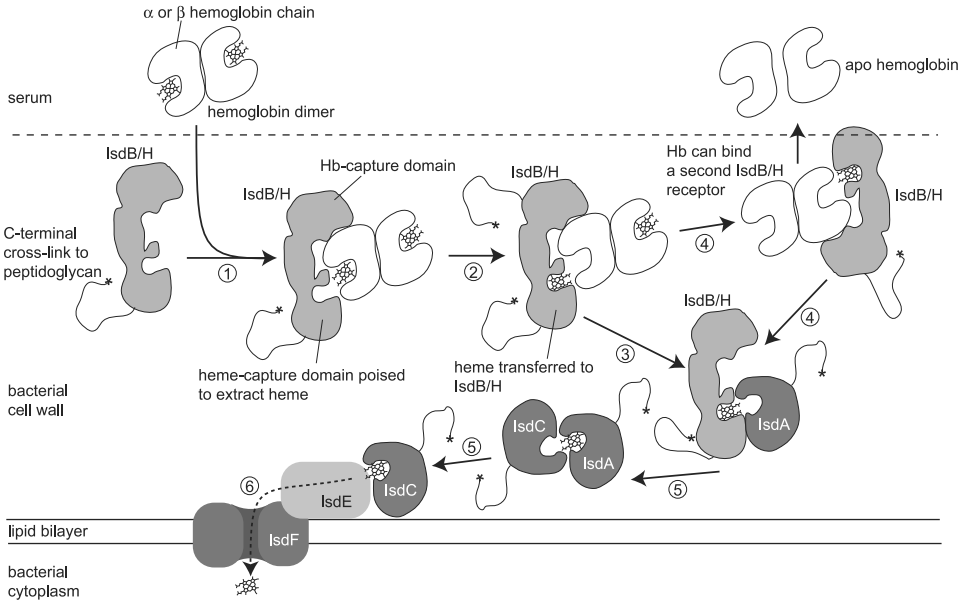

FIGURE 6. **Model of heme extraction from human Hb by the *S. aureus* Hb receptors IsdB and IsdH.** Hb is bound, through α or β subunits, by the Hb capture domain of IsdH/B (*step 1*). An α·β Hb dimer is shown here, but we envisage that the receptor could equally bind to Hb tetramer or individual α/β Hb monomers. Heme is transferred from the α/β chain to the heme acceptor domain of IsdH/B, which is positioned over the globin heme pocket (*step 2*). IsdH/B that dissociates from Hb in the heme-loaded form interacts transiently with, and transfers heme to, IsdA (*step 3*) (16, 18) or IsdC (not shown). Hb may interact sequentially or simultaneously with other IsdH/B receptors until all heme groups are removed and transferred to IsdA/C (*step 4*). IsdC can receive heme from IsdA (36), or directly from IsdB/H (16, 18), and delivers heme to the ligand-binding subunit (IsdE, *step 5*) (18) of the heme permease (IsdF), which shuttles heme to the cytoplasm (*step 6*).

domains are identified as heme-binding modules, based on conservation of key residues involved in heme interactions. The most conserved NEAT-containing protein is IsdC. IsdC contains a single NEAT domain that delivers heme to the heme permease complex in the cytoplasmic membrane (IsdE/F), which is also highly conserved in *Firmicutes*, suggesting that IsdC/E/F are components of an ancestral heme-scavenging pathway. In contrast, upstream of IsdC, there is variation in the number of NEAT proteins and the domain architectures of these proteins in different bacterial species, reflecting diversification in the mechanisms for heme capture and heme relay to IsdC. NEAT domain proteins that target Hb as an iron source include IsdX1, IsdX2, and Hal from *B. anthracis* (30–33), IlsA from *B. cereus* (34), and Shr from *S. pyogenes* (35, 68). Each of these proteins contains one or more heme-binding NEAT domains and additional domains with poorly characterized function (Fig. 7). Interestingly, the diverse domain architecture suggests that heme capture from Hb may have evolved multiple times. Although the $IsdH^{N2}$ and linker domain sequences appear to be unique to *S. aureus* and closely related species, different domains could play conceptually similar roles to target and support heme-binding NEAT domains. For example, in Shr, sequences adjacent to the N-terminal NEAT domain have been implicated in Hb binding (68). The structures and properties of these domains have not been determined. In addition, Shr, IlsA, and Hal contain leucine-rich repeat domains; these domains are well established as versatile protein interaction motifs (69). The secreted hemophore IsdX2 takes heme from Hb via four heme-binding NEAT domains (32, 33). A fifth NEAT domain does not bind heme, but does interact with Hb (32), and so may play structural or Hb-targeting function in the context of the full-length IsdX2. $IsdH^{N2\text{-}N3}$ is the first example

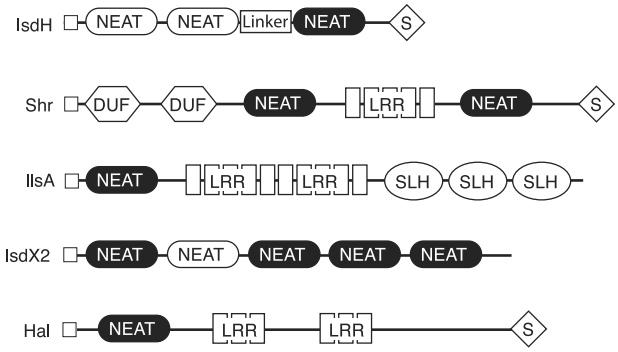

FIGURE 7. **Domain structure of Hb-binding proteins from bacterial species belonging to the phylum *Firmicutes*.** The domain structures of Hb-binding proteins from Gram-positive bacteria: IsdH, Shr (*S. pyogenes*), IlsA (*B. cereus*), IsdX2 (*B. anthracis*), and Hal (*B. anthracis*). Signal peptides direct secretion (*open squares*) and anchoring to the peptidoglycal cell wall (*S*). S-layer homology domain (*SLH*) mediates attachment to a proteinaceous layer on the outer surface of the cell wall. A subset of NEAT domains mediates heme binding (*black background*), whereas others may have either protein binding or structural functions (*white background*). Domains with unknown function (*DUF*) and leucine-rich repeats (*LRR*) are present in some Hb-binding proteins.

from Gram-positive bacteria where a structure comprising multiple domains of an Hb receptor has been determined, revealing how these domains cooperate to achieve function.

The $IsdH^{N2\text{-}N3}$·Hb structure predicts that IsdH can access iron from all forms of Hb that are likely to be encountered in serum following erythrocyte lysis. Dissociation of the Hb tetramer occurs *in vivo* following erythrocyte lysis, due to dilution effects and autooxidation processes. In addition, removal of heme from one or more globin chains is expected to destabilize Hb, leading to increased formation of monomers (27, 42). Importantly, our results suggest that a similar mechanism of heme extraction will operate for tetramer, dimer, or monomer

globin species. Hb released by hemolysis is also bound by the serum scavenger protein haptoglobin, which inhibits globin denaturation and targets Hb to the scavenger receptor CD163 on macrophages. IsdB/H binds Hb·haptoglobin complexes and the $IsdH^{N1}$ domain is reported to bind haptoglobin and hemoglobin independently (7, 10, 12, 22), but heme uptake from Hb·haptoglobin complexes has not been measured. The structure of an Hb·haptoglobin complex was solved recently (70), and comparison of that structure with the $IsdH^{N2\text{-}N3}$·Hb complex shows that haptoglobin does not block $IsdH^{N2}$ or $IsdH^{N3}$ domain interactions with the globin, suggesting that Hb·haptoglobin is available as an iron source for *S. aureus*.

In summary, our data reveal the mechanism by which *S. aureus*, an important human pathogen, obtains the iron that is essential for infection. The pre-organized, multidomain architecture of the IsdH/B heme-capturing unit is a solution that couples highly specific recognition of Hb to a functional heme extraction module and might represent a general strategy exploited by a wide range of pathogenic bacteria.

Acknowledgments—We thank the staff of the MX beam lines at the Australian Synchrotron for help with data collection.

REFERENCES

1. Klevens, R. M., Morrison, M. A., Nadle, J., Petit, S., Gershman, K., Ray, S., Harrison, L. H., Lynfield, R., Dumyati, G., Townes, J. M., Craig, A. S., Zell, E. R., Fosheim, G. E., McDougal, L. K., Carey, R. B., and Fridkin, S. K. (2007) Invasive methicillin-resistant *Staphylococcus aureus* infections in the United States. *JAMA* **298,** 1763–1771
2. Klein, E., Smith, D. L., and Laxminarayan, R. (2007) Hospitalizations and deaths caused by methicillin-resistant *Staphylococcus aureus*, United States, 1999–2005. *Emerg. Infect. Dis.* **13,** 1840–1846
3. Dukic, V. M., Lauderdale, D. S., Wilder, J., Daum, R. S., and David, M. Z. (2013) Epidemics of community-associated methicillin-resistant *Staphylococcus aureus* in the United States: a meta-analysis. *PLoS One* **8,** e52722
4. Nairz, M., Schroll, A., Sonnweber, T., and Weiss, G. (2010) The struggle for iron - a metal at the host-pathogen interface. *Cell. Microbiol.* **12,** 1691–1702
5. Torres, V. J., Attia, A. S., Mason, W. J., Hood, M. I., Corbin, B. D., Beasley, F. C., Anderson, K. L., Stauff, D. L., McDonald, W. H., Zimmerman, L. J., Friedman, D. B., Heinrichs, D. E., Dunman, P. M., and Skaar, E. P. (2010) *Staphylococcus aureus* fur regulates the expression of virulence factors that contribute to the pathogenesis of pneumonia. *Infect. Immun.* **78,** 1618–1628
6. Noinaj, N., Easley, N. C., Oke, M., Mizuno, N., Gumbart, J., Boura, E., Steere, A. N., Zak, O., Aisen, P., Tajkhorshid, E., Evans, R. W., Gorringe, A. R., Mason, A. B., Steven, A. C., and Buchanan, S. K. (2012) Structural basis for iron piracy by pathogenic *Neisseria*. *Nature* **483,** 53–58
7. Dryla, A., Gelbmann, D., von Gabain, A., and Nagy, E. (2003) Identification of a novel iron regulated staphylococcal surface protein with haptoglobin-haemoglobin binding activity. *Mol. Microbiol.* **49,** 37–53
8. Skaar, E. P., Humayun, M., Bae, T., DeBord, K. L., and Schneewind, O. (2004) Iron-source preference of *Staphylococcus aureus* infections. *Science* **305,** 1626–1628
9. Torres, V. J., Pishchany, G., Humayun, M., Schneewind, O., and Skaar, E. P. (2006) *Staphylococcus aureus* IsdB is a hemoglobin receptor required for heme iron utilization. *J. Bacteriol.* **188,** 8421–8429
10. Dryla, A., Hoffmann, B., Gelbmann, D., Giefing, C., Hanner, M., Meinke, A., Anderson, A. S., Koppensteiner, W., Konrat, R., von Gabain, A., and Nagy, E. (2007) High-affinity binding of the staphylococcal HarA protein to haptoglobin and hemoglobin involves a domain with an antiparallel eight-stranded β-barrel fold. *J. Bacteriol.* **189,** 254–264
11. Krishna Kumar, K., Jacques, D. A., Pishchany, G., Caradoc-Davies, T., Spirig, T., Malmirchegini, G. R., Langley, D. B., Dickson, C. F., Mackay, J. P., Clubb, R. T., Skaar, E. P., Guss, J. M., and Gell, D. A. (2011) Structural basis for hemoglobin capture by *Staphylococcus aureus* cell-surface protein, IsdH. *J. Biol. Chem.* **286,** 38439–38447
12. Pilpa, R. M., Robson, S. A., Villareal, V. A., Wong, M. L., Phillips, M., and Clubb, R. T. (2009) Functionally distinct NEAT (NEAr Transporter) domains within the *Staphylococcus aureus* IsdH/HarA protein extract heme from methemoglobin. *J. Biol. Chem.* **284,** 1166–1176
13. Pishchany, G., McCoy, A. L., Torres, V. J., Krause, J. C., Crowe, J. E., Jr., Fabry, M. E., and Skaar, E. P. (2010) Specificity for human hemoglobin enhances *Staphylococcus aureus* infection. *Cell Host Microbe* **8,** 544–550
14. Abe, R., Caaveiro, J. M., Kozuka-Hata, H., Oyama, M., and Tsumoto, K. (2012) Mapping ultra-weak protein-protein interactions between heme transporters of *Staphylococcus aureus*. *J. Biol. Chem.* **287,** 16477–16487
15. Mack, J., Vermeiren, C., Heinrichs, D. E., and Stillman, M. J. (2004) *In vivo* heme scavenging by *Staphylococcus aureus* IsdC and IsdE proteins. *Biochem. Biophys. Res. Commun.* **320,** 781–788
16. Muryoi, N., Tiedemann, M. T., Pluym, M., Cheung, J., Heinrichs, D. E., and Stillman, M. J. (2008) Demonstration of the iron-regulated surface determinant (Isd) heme transfer pathway in *Staphylococcus aureus*. *J. Biol. Chem.* **283,** 28125–28136
17. Tiedemann, M. T., Heinrichs, D. E., and Stillman, M. J. (2012) The multiprotein heme shuttle pathway in *Staphylococcus aureus*: Isd cog-wheel kinetics. *J. Am. Chem. Soc.* **134,** 16578–16585
18. Zhu, H., Xie, G., Liu, M., Olson, J. S., Fabian, M., Dooley, D. M., and Lei, B. (2008) Pathway for heme uptake from human methemoglobin by the iron-regulated surface determinants system of *Staphylococcus aureus*. *J. Biol. Chem.* **283,** 18450–18460
19. Mazmanian, S. K., Skaar, E. P., Gaspar, A. H., Humayun, M., Gornicki, P., Jelenska, J., Joachmiak, A., Missiakas, D. M., and Schneewind, O. (2003) Passage of heme-iron across the envelope of *Staphylococcus aureus*. *Science* **299,** 906–909
20. Morrissey, J. A., Cockayne, A., Hammacott, J., Bishop, K., Denman-Johnson, A., Hill, P. J., and Williams, P. (2002) Conservation, surface exposure, and *in vivo* expression of the Frp family of iron-regulated cell wall proteins in *Staphylococcus aureus*. *Infect. Immun.* **70,** 2399–2407
21. Hempel, K., Herbst, F. A., Moche, M., Hecker, M., and Becher, D. (2011) A quantitative proteomic view on secreted, cell surface-associated and cytoplasmic proteins of the methicillin-resistant human pathogen *Staphylococcus aureus* under iron-limited conditions. *J. Proteome Res.* **10,** 1657–1666
22. Visai, L., Yanagisawa, N., Josefsson, E., Tarkowski, A., Pezzali, I., Rooijakkers, S. H., Foster, T. J., and Speziale, P. (2009) Immune evasion by *Staphylococcus aureus* conferred by iron-regulated surface determinant protein IsdH. *Microbiology* **155,** 667–679
23. Pishchany, G., Dickey, S. E., and Skaar, E. P. (2009) Subcellular localization of the *Staphylococcus aureus* heme iron transport components IsdA and IsdB. *Infect. Immun.* **77,** 2624–2634
24. Cheng, A. G., Kim, H. K., Burts, M. L., Krausz, T., Schneewind, O., and Missiakas, D. M. (2009) Genetic requirements for *Staphylococcus aureus* abscess formation and persistence in host tissues. *FASEB J.* **23,** 3393–3404
25. del Rio, A., Cervera, C., Moreno, A., Moreillon, P., and Miró, J. M. (2009) Patients at risk of complications of *Staphylococcus aureus* bloodstream infection. *Clin. Infect. Dis.* **48,** Suppl. 4, S246–S253
26. Miro, J. M., Anguera, I., Cabell, C. H., Chen, A. Y., Stafford, J. A., Corey, G. R., Olaison, L., Eykyn, S., Hoen, B., Abrutyn, E., Raoult, D., Bayer, A., and Fowler, V. G., Jr. (2005) *Staphylococcus aureus* native valve infective endocarditis: report of 566 episodes from the International Collaboration on Endocarditis Merged Database. *Clin. Infect. Dis.* **41,** 507–514
27. Spirig, T., Malmirchegini, G. R., Zhang, J., Robson, S. A., Sjodt, M., Liu, M., Krishna Kumar, K., Dickson, C. F., Gell, D. A., Lei, B., Loo, J. A., and Clubb, R. T. (2013) *Staphylococcus aureus* uses a novel multi-domain receptor to break apart human hemoglobin and steal its heme. *J. Biol. Chem.* **288,** 1065–1078
28. Zapotoczna, M., Heilbronner, S., Speziale, P., and Foster, T. J. (2012) Iron regulated surface determinant (Isd) proteins of Staphylococcus lugdunensis. *J. Bacteriol.* **194,** 6453–6467
29. Anguera, I., Del Río, A., Miró, J. M., Matínez-Lacasa, X., Marco, F., Gumá,

J. R., Quaglio, G., Claramonte, X., Moreno, A., Mestres, C. A., Mauri, E., Azqueta, M., Benito, N., García-de la María, C., Almela, M., Jiménez-Expósito, M. J., Sued, O., De Lazzari, E., and Gatell, J. M. (2005) Staphylococcus lugdunensis infective endocarditis: description of 10 cases and analysis of native valve, prosthetic valve, and pacemaker lead endocarditis clinical profiles. *Heart* **91,** e10

30. Balderas, M. A., Nobles, C. L., Honsa, E. S., Alicki, E. R., and Maresso, A. W. (2012) Hal Is a *Bacillus anthracis* heme acquisition protein. *J. Bacteriol.* **194,** 5513–5521
31. Ekworomadu, M. T., Poor, C. B., Owens, C. P., Balderas, M. A., Fabian, M., Olson, J. S., Murphy, F., Balkabasi, E., Honsa, E. S., He, C., Goulding, C. W., and Maresso, A. W. (2012) Differential function of lip residues in the mechanism and biology of an anthrax hemophore. *PLoS Pathog.* **8,** e1002559
32. Honsa, E. S., Fabian, M., Cardenas, A. M., Olson, J. S., and Maresso, A. W. (2011) The five near-iron transporter (NEAT) domain anthrax hemophore, IsdX2, scavenges heme from hemoglobin and transfers heme to the surface protein IsdC. *J. Biol. Chem.* **286,** 33652–33660
33. Honsa, E. S., Owens, C. P., Goulding, C. W., and Maresso, A. W. (2013) The near-iron transporter (NEAT) domains of the anthrax hemophore IsdX2 require a critical glutamine to extract heme from methemoglobin. *J. Biol. Chem.* **288,** 8479–8490
34. Daou, N., Buisson, C., Gohar, M., Vidic, J., Bierne, H., Kallassy, M., Lereclus, D., and Nielsen-LeRoux, C. (2009) IlsA, a unique surface protein of *Bacillus cereus* required for iron acquisition from heme, hemoglobin and ferritin. *PLoS Pathog.* **5,** e1000675
35. Ouattara, M., Pennati, A., Devlin, D. J., Huang, Y. S., Gadda, G., and Eichenbaum, Z. (2013) Kinetics of heme transfer by the Shr NEAT domains of Group A *Streptococcus*. *Arch. Biochem. Biophys.* **538,** 71–79
36. Liu, M., Tanaka, W. N., Zhu, H., Xie, G., Dooley, D. M., and Lei, B. (2008) Direct hemin transfer from IsdA to IsdC in the iron-regulated surface determinant (Isd) heme acquisition system of *Staphylococcus aureus*. *J. Biol. Chem.* **283,** 6668–6676
37. Moriwaki, Y., Caaveiro, J. M., Tanaka, Y., Tsutsumi, H., Hamachi, I., and Tsumoto, K. (2011) Molecular basis of recognition of antibacterial porphyrins by heme-transporter IsdH-NEAT3 of *Staphylococcus aureus*. *Biochemistry* **50,** 7311–7320
38. Vu, N. T., Moriwaki, Y., Caaveiro, J. M., Terada, T., Tsutsumi, H., Hamachi, I., Shimizu, K., and Tsumoto, K. (2013) Selective binding of antimicrobial porphyrins to the heme-receptor IsdH-NEAT3 of *staphylococcus aureus*. *Protein Sci.* **22,** 942–953
39. Gaudin, C. F. M., Grigg, J. C., Arrieta, A. L., and Murphy, M. E. P. (2011) Unique heme-iron coordination by the hemoglobin receptor IsdB of *Staphylococcus aureus*. *Biochemistry* **50,** 5443–5452
40. Grigg, J. C., Mao, C. X., and Murphy, M. E. (2011) Iron-coordinating tyrosine is a key determinant of NEAT domain heme transfer. *J. Mol. Biol.* **413,** 684–698
41. Villareal, V. A., Spirig, T., Robson, S. A., Liu, M., Lei, B., and Clubb, R. T. (2011) Transient weak protein-protein complexes transfer heme across the cell wall of *Staphylococcus aureus*. *J. Am. Chem. Soc.* **133,** 14176–14179
42. Hargrove, M. S., Whitaker, T., Olson, J. S., Vali, R. J., and Mathews, A. J. (1997) Quaternary structure regulates hemin dissociation from human hemoglobin. *J. Biol. Chem.* **272,** 17385–17389
43. Watanabe, M., Tanaka, Y., Suenaga, A., Kuroda, M., Yao, M., Watanabe, N., Arisaka, F., Ohta, T., Tanaka, I., and Tsumoto, K. (2008) Structural basis for multimeric heme complexation through a specific protein-heme interaction: the case of the third neat domain of IsdH from *Staphylococcus aureus*. *J. Biol. Chem.* **283,** 28649–28659
44. Otwinowski, Z., and Minor, W. (1997) Processing of x-ray diffraction data collected in oscillation mode. *Methods Enzymol.* **276,** 307–326
45. McCoy, A. J., Grosse-Kunstleve, R. W., Adams, P. D., Winn, M. D., Storoni, L. C., and Read, R. J. (2007) Phaser crystallographic software. *J. Appl. Crystallogr.* **40,** 658–674
46. Stein, N. (2008) CHAINSAW: a program for mutating pdb files used as templates in molecular replacement. *J. Appl. Crystallogr.* **41,** 641–643
47. Murshudov, G. N., Vagin, A. A., and Dodson, E. J. (1997) Refinement of macromolecular structures by the maximum-likelihood method. *Acta Crystallogr. D Biol. Crystallogr.* **53,** 240–255
48. Emsley, P., and Cowtan, K. (2004) Coot: model-building tools for molecular graphics. *Acta Crystallogr. D Biol. Crystallogr.* **60,** 2126–2132
49. Chen, V. B., Arendall, W. B., 3rd, Headd, J. J., Keedy, D. A., Immormino, R. M., Kapral, G. J., Murray, L. W., Richardson, J. S., and Richardson, D. C. (2010) MolProbity: all-atom structure validation for macromolecular crystallography. *Acta Crystallogr. D Biol. Crystallogr.* **66,** 12–21
50. Bricogne, G., Blanc, E., Brandl, M., Flensburg, C., Keller, P., Paciorek, M., Roversi, P., Sharff, A., Smart, O. S., Vonrhein, C., and Womack, T. O. (2011) *BUSTER*, version 2.10.0, Global Phasing Ltd., Cambridge, UK
51. Smart, O. S., Womack, T. O., Flensburg, C., Keller, P., Paciorek, W., Sharff, A., Vonrhein, C., and Bricogne, G. (2012) Exploiting structure similarity in refinement: automated NCS and target-structure restraints in BUSTER. *Acta Crystallogr. D Biol. Crystallogr.* **68,** 368–380
52. Jacques, D. A., and Trewhella, J. (2010) Small-angle scattering for structural biology–expanding the frontier while avoiding the pitfalls. *Protein Sci.* **19,** 642–657
53. Volkov, V. V., and Svergun, D. I. (2003) Uniqueness of *ab initio* shape determination in small-angle scattering. *J. Appl. Crystallogr.* **36,** 860–864
54. Franke, D., and Svergun, D. I. (2009) DAMMIF, a program for rapid *ab initio* shape determination in small-angle scattering. *J. Appl. Crystallogr.* **42,** 343–346
55. Kozin, M., and Svergun, D. I. (2001) Automated matching of high- and low-resolution structural models. *J. Appl. Crystallogr.* **34,** 33–41
56. Ascoli, F., Fanelli, M. R., and Antonini, E. (1981) Preparation and properties of apohemoglobin and reconstituted hemoglobins. *Methods Enzymol.* **76,** 72–87
57. Park, S. Y., Yokoyama, T., Shibayama, N., Shiro, Y., and Tame, J. R. (2006) 1.25 Å resolution crystal structures of human haemoglobin in the oxy, deoxy and carbonmonoxy forms. *J. Mol. Biol.* **360,** 690–701
58. Yi, J., Thomas, L. M., and Richter-Addo, G. B. (2011) Structure of human R-state aquomethemoglobin at 2.0 Å resolution. *Acta Crystallogr. Sect. F Struct. Biol. Cryst. Commun.* **67,** 647–651
59. Svergun, D., Barberato, C., and Koch, M. H. J. (1995) CRYSOL - a program to evaluate x-ray solution scattering of biological macromolecules from atomic coordinates. *J. Appl. Crystallogr.* **28,** 768–773
60. Banci, L., Bertini, I., Cantini, F., Felli, I. C., Gonnelli, L., Hadjiliadis, N., Pierattelli, R., Rosato, A., and Voulgaris, P. (2006) The Atx1-Ccc2 complex is a metal-mediated protein-protein interaction. *Nat. Chem. Biol.* **2,** 367–368
61. Crowley, P. B., and Ubbink, M. (2003) Close encounters of the transient kind: protein interactions in the photosynthetic redox chain investigated by NMR spectroscopy. *Acc. Chem. Res.* **36,** 723–730
62. Bauer, J., Reiss, K., Veerabagu, M., Heunemann, M., Harter, K., and Stehle, T. (2013) Structure-function analysis of Arabidopsis thaliana histidine kinase AHK5 bound to its cognate phosphotransfer protein AHP1. *Mol. Plant* **6,** 959–970
63. Zhao, X., Copeland, D. M., Soares, A. S., and West, A. H. (2008) Crystal structure of a complex between the phosphorelay protein YPD1 and the response regulator domain of SLN1 bound to a phosphoryl analog. *J. Mol. Biol.* **375,** 1141–1151
64. Zapf, J., Sen, U., Madhusudan, Hoch, J. A., and Varughese, K. I. (2000) A transient interaction between two phosphorelay proteins trapped in a crystal lattice reveals the mechanism of molecular recognition and phosphotransfer in signal transduction. *Structure* **8,** 851–862
65. Eliezer, D., and Wright, P. E. (1996) Is apomyoglobin a molten globule? Structural characterization by NMR. *J. Mol. Biol.* **263,** 531–538
66. Nepluev, I., Afonina, G., Fusco, W. G., Leduc, I., Olsen, B., Temple, B., and Elkins, C. (2009) An immunogenic, surface-exposed domain of *Haemophilus ducreyi* outer membrane protein HgbA is involved in hemoglobin binding. *Infect. Immun.* **77,** 3065–3074
67. Fusco, W. G., Choudhary, N. R., Council, S. E., Collins, E. J., and Leduc, I. (2013) Mutational analysis of hemoglobin binding and heme utilization by a bacterial hemoglobin receptor. *J. Bacteriol.* **195,** 3115–3123
68. Ouattara, M., Cunha, E. B., Li, X., Huang, Y. S., Dixon, D., and Eichenbaum, Z. (2010) Shr of Group A *Streptococcus* is a new type of composite NEAT protein involved in sequestering heme from methemoglobin. *Mol. Microbiol.* **78,** 739–756

69. Kobe, B., and Kajava, A. V. (2001) The leucine-rich repeat as a protein recognition motif. *Curr. Opin. Struct. Biol.* **11,** 725–732
70. Andersen, C. B., Torvund-Jensen, M., Nielsen, M. J., de Oliveira, C. L., Hersleth, H. P., Andersen, N. H., Pedersen, J. S., Andersen, G. R., and Moestrup, S. K. (2012) Structure of the haptoglobin-haemoglobin complex. *Nature* **489,** 456–459
71. Silva, M. M., Rogers, P. H., and Arnone, A. (1992) A third quaternary structure of human hemoglobin A at 1.7-A resolution. *J. Biol. Chem.* **267,** 17248–17256
72. Konarev, P. V., Volkov, V. V., Sokolova, A. V., Koch, M. H., and Svergun, D. I. (2003) PRIMUS: a Windows PC-based system for small-angle scattering data analysis. *J. Appl. Crystallogr.* **36,** 1277–1282